NASA TECHNICAL NOTE

NASA TN D-3851

NASA TN D-3851

CALCULATION OF THE CENTERED ONE-DIMENSIONAL UNSTEADY EXPANSION OF A REACTING GAS MIXTURE SUBJECT TO VIBRATIONAL AND CHEMICAL NONEQUILIBRIUM

by Laurence N. Connor, Jr.

Langley Research Center
Langley Station, Hampton, Va.

NATIONAL AERONAUTICS AND SPACE ADMINISTRATION • WASHINGTON, D. C. • FEBRUARY 1967

NASA TN D-3851

CALCULATION OF THE CENTERED ONE-DIMENSIONAL UNSTEADY EXPANSION OF A REACTING GAS MIXTURE SUBJECT TO VIBRATIONAL AND CHEMICAL NONEQUILIBRIUM

By Laurence N. Connor, Jr.

Langley Research Center
Langley Station, Hampton, Va.

NATIONAL AERONAUTICS AND SPACE ADMINISTRATION

For sale by the Clearinghouse for Federal Scientific and Technical Information
Springfield, Virginia 22151 – Price $2.00

CALCULATION OF THE CENTERED ONE-DIMENSIONAL UNSTEADY EXPANSION OF A REACTING GAS MIXTURE SUBJECT TO VIBRATIONAL AND CHEMICAL NONEQUILIBRIUM

By Laurence N. Connor, Jr.
Langley Research Center

SUMMARY

A method of calculation based on a previously developed method-of-characteristics approach is presented for use in analyzing the nonequilibrium one-dimensional unsteady expansion of a reacting mixture of gases. The characteristic equations are written in a general form which permits the consideration of a number of rate processes. A multicomponent gas model with a number of simultaneous rate processes is used, and both chemical and vibrational nonequilibrium are permitted. A procedure which utilizes the method of characteristics in a Lagrangian frame of reference is programed to yield solutions on the IBM 7094 electronic data processing system. Calculations are presented for a typical unsteady expansion to demonstrate the use of the program.

INTRODUCTION

The one-dimensional unsteady expansion has recently assumed new importance in the operation cycle of facilities designed to produce high-enthalpy flow for reentry simulation and chemical kinetic studies. The expansion tube discussed in references 1 and 2 is designed to produce high-velocity flow for reentry simulation. In the operating cycle of the expansion tube an unsteady expansion is used to accelerate the test gas. This expansion is a critical phase in the expansion-tube cycle since any deviation from equilibium at this point will alter the final state of the test gas. The need for a solution which is capable of completely evaluating the unsteady expansion is therefore apparent.

For high-enthalpy gas flow, the role of chemical kinetics assumes new importance. In order to analyze such flow accurately, a knowledge of the rates of the reactions involved is necessary. The unsteady expansion can provide a means of processing a gas to establish conditions under which chemical recombination rates can be directly measured. Such an application of the unsteady expansion is discussed in references 3, 4, and 5. The operating conditions involve temperatures and pressures at which internal energy excitation and dissociation of the molecular species of the processed gas occur. The rate at which these processes occur appreciably affects the flow properties of the gas processed by the

expansion. An analysis of the unsteady expansion in which rate-controlled phenomena can be included and for which the effects of such processes can be ascertained is therefore required.

The first approach to predicting the structure of a nonequilibrium unsteady expansion is found in reference 6. A centered rarefaction wave in which only vibrational nonequilibrium is present is treated. That work was extended in references 7 and 8 by introducing the "ideal dissociating gas" of references 9 and 10 into the treatment of dissociative nonequilibrium. The calculation procedure and computed results for the unsteady expansion of a vibrationally relaxing nitrogen-oxygen mixture are presented in reference 11. The numerical approach, originated in reference 6 and used in references 7 and 11, is utilized in the present work.

The basic objective of the present investigation is to provide an analysis of the one-dimensional unsteady expansion of a reacting mixture of gases subject to vibrational and dissociative nonequilibrium. The physical model of the expansion is the constant-velocity withdrawal of a piston from a cylinder of gas which is initially in chemical equilibrium. The chemistry and thermodynamics of the problem are formulated generally so that various gas mixtures and reactions may be considered. The equations of motion governing an unsteady expansion are used to establish characteristic lines and compatibility relations along the lines.

A procedure is established for calculation of the flow field by the method of characteristics and is them programed in FORTRAN language to yield solutions on the IBM 7094 electronic data processing system. The solution of a typical unsteady expansion in an oxygen-nitrogen mixture is presented to illustrate the general structure of such an expansion. The variations of thermodynamic properties, velocities, and compositions through the expansion fan are depicted for gas particles having different residence times in the expansion, and thus the effects of nonequilibrium on the expansion are illustrated.

SYMBOLS

A_1, A_2, A_3	dimensionless parameters defined by equation (18)
A_i, B_i, C_i	constants used in vibrational-relaxation-time expressions
a	speed of sound
b	Lagrangian coordinate denoting a fixed mass element
D_j, E_j, F_j	chemical rate constants

e	internal energy per unit mass
f_i	factor used to provide exclusion and inclusion of rotational energy of monatomic and diatomic molecules, respectively ($f_i = 0$ for monatomic molecule; $f_i = 1$ for diatomic molecule)
h	enthalpy per unit mass
i	species identification
j	reaction identification
K	total number of rate-controlled variables
k	rate-controlled-variable identification
k_j	specific reaction rate coefficient for jth reaction
M	catalytic species in chemical reaction
m	total number of reactions
n	total number of species
N_o	Avogadro number
p	pressure
q	rate-controlled variable considered in appendix A
q_k	general rate-controlled variable ($k = 1, \ldots, K$)
R	universal gas constant
T	translational temperature
t	time
t'	reference time

U	piston velocity
u	velocity
x	position coordinate of fluid particle
x_i	mass fraction of ith species for $i = 1, \ldots, n$ (x_O represents the mass fraction of atomic oxygen)
y	modified Lagrangian coordinate, b/t
γ	frozen specific heat ratio of the undisturbed gas
Δ_i	heat of formation of ith species, energy per molecule
θ_i	characteristic vibrational temperature of ith species
μ	molecular weight of mixture
μ_i	molecular weight of ith species
ν_{ij}	stoichiometric coefficient of ith species of reactant in jth reaction
ν'_{ij}	stoichiometric coefficient of ith species of product in jth reaction
ρ	density
σ_i	vibrational energy per mole of ith species for $i = 1, \ldots, n$ (σ_{N_2} and σ_{O_2} represent vibrational energies of N_2 and O_2, respectively)
τ_i	vibrational relaxation time of ith species
ω	rate of change of rate-controlled variable q
ω_k	rate of change of kth rate-controlled variable

Subscripts:

A,B,C,D,P	points in calculation procedure defined in figure 9
AP,BP,DP	denote average of values at two grid points

c	required for complete frozen expansion to $p = 0$
eq	equilibrium conditions
f	results for frozen flow
n	evaluated at intermediate condition (fig. 1)
o	initial condition in undisturbed gas
p	evaluated with pressure held constant
q	evaluated with rate-controlled variables in appendix A held constant
q_k	evaluated with rate-controlled variable held constant
ρ	evaluated with density held constant
+,-,0	characteristic directions

A bar over a symbol denotes a nondimensional quantity.

THEORETICAL DEVELOPMENT

Physical Model of Expansion

A physical picture of a centered one-dimensional unsteady expansion can be obtained by considering figure 1. For illustrative purposes the structure of the expansion is shown for a perfect gas. A semi-infinite reservior of constant cross-sectional area contains a gas mixture assumed to be in a state of chemical and thermodynamic equilibrium. At time zero, the piston is withdrawn with constant velocity, and a rarefaction wave which propagates into the gas in the reservoir is produced.

The expansion can be divided into two regions. The first is referred to as the expansion fan. In this region, temperatures and pressures decrease rapidly during the passage of the rarefaction wave. If the reservoir gas exists initially in a dissociated state, the atoms must recombine as they are processed by the expansion if chemical equilibrium is to be maintained. In like manner, the vibrational energy must decrease. Both of these phenomena are controlled by rate processes.

The effects of rate processes can be understood by considering the different particle paths in figure 1. Path I represents a particle which is very near the piston face initially.

Its residence time in the expansion fan is very short and the rate-controlled quantities have insufficient time for adjustment to equilibrium. Since very little adjustment occurs, the particle essentially experiences a frozen expansion. Particle III has a relatively long residence time in the expansion and the rate processes are permitted adequate time for the flow to relax to equilibrium. Such a particle undergoes an equilibrium expansion. The energy contained in dissociation is returned to the translational and rotational energy modes of the gas. Particle path II represents nonequilibrium flow, an intermediate region between the two extremes. The residence time is of a magnitude that allows some relaxation of the rate-controlled quantities toward equilibrium. The present investigation is directed toward the analysis of this nonequilibrium region.

Governing Equations

The Lagrangian coordinate system can be used effectively in the present problem. Such a system has the advantage of readily establishing a particle path along which the rate and energy equations can be applied. In the Lagrangian frame of reference, attention is given to what happens to each individual fluid particle in the course of time. Each fluid particle must therefore be labeled. This labeling is accomplished by designating each particle according to its position coordinate x in the x-t plane at some reference time $t = t_0$. This value is called b, the Lagrangian coordinate specifying the particle being considered. The two independent variables in the Lagrangian system are therefore b and t.

Flow equations.- The equations expressing the conservation of mass, momentum, and energy for one-dimensional unsteady expansion in the Lagrangian coordinate system are presented in references 12 and 6 and are as follows:

$$\frac{\partial u}{\partial b} + \frac{\rho_0}{\rho^2}\frac{\partial \rho}{\partial t} = 0 \tag{1}$$

$$\frac{\partial u}{\partial t} + \frac{1}{\rho_0}\frac{\partial p}{\partial b} = 0 \tag{2}$$

and

$$\frac{\partial h}{\partial t} - \frac{1}{\rho}\frac{\partial p}{\partial t} = 0 \tag{3}$$

Equation of state.- The state of the reacting gas mixture can be expressed in the general form

$$h = h\left(p,\rho,q_1,\ldots,q_K\right) \tag{4}$$

The variables denoted by q_k for $k = 1,\ldots,K$ are used to specify the vibrational energy and/or the chemical state of the gas. In actuality, these variables express the vibrational energy and/or the mass fraction of each component species in the gas mixture, that is,

$$\left.\begin{aligned} q_1 = \sigma_1, \quad q_2 = \sigma_2, \quad \ldots, \quad q_n = \sigma_n \\ q_{n+1} = x_1, \quad q_{n+2} = x_2, \quad \ldots, \quad q_{2n} = x_n \end{aligned}\right\} \tag{5}$$

where σ_i is the vibrational energy per mole of the ith species for $i = 1,\ldots,n$, x_i is the mass fraction of the ith species for $i = 1,\ldots,n$, n is the total number of species, and K is the number of nonequilibrium variables ($K = 2n$). For convenience in handling the equations in the present paper q_k is used to represent the vibrational and dissociative state of the gas. When more detailed operations are required, equation (5) is introduced so that each variable can be treated in the proper manner.

Rate equations.- For the nonequilibrium expansion, the value of q_k at any point in the flow depends on the rate equations and the process which the gas has undergone. The rate equations can be expressed in the general form

$$\frac{\partial q_k}{\partial t} = \omega_k \tag{6}$$

where

$$\omega_k = \omega_k\left(p,\rho,q_1,\ldots,q_K\right)$$

and are subsequently presented in detail for each rate process considered.

Characteristic Equations

The characteristic equations in the Lagrangian coordinate system are derived in appendix A. Along the + and - characteristic lines

$$\left.\begin{aligned} \left(\frac{db}{dt}\right)_+ &= \frac{\rho a_f}{\rho_o} \\ \left(\frac{db}{dt}\right)_- &= -\frac{\rho a_f}{\rho_o} \end{aligned}\right\} \tag{7}$$

the respective compatibility relations are

$$\left.\begin{aligned} \frac{dp}{dt} + \rho a_f \frac{du}{dt} - a_f{}^2 \frac{\sum_{k=1}^{K} \frac{\partial h}{\partial q_k} \omega_k}{\frac{\partial h}{\partial \rho}} = 0 \\ \frac{dp}{dt} - \rho a_f \frac{du}{dt} - a_f{}^2 \frac{\sum_{k=1}^{K} \frac{\partial h}{\partial q_k} \omega_k}{\frac{\partial h}{\partial \rho}} = 0 \end{aligned}\right\} \tag{8}$$

The particle path in the Lagrangian system is given by

$$\left(\frac{db}{dt}\right)_0 = 0 \tag{9}$$

and, along this path, both the energy equation

$$\frac{dh}{dt} - \frac{1}{\rho}\frac{dp}{dt} = 0 \tag{10}$$

and the rate equation

$$\frac{dq_k}{dt} = \omega_k \tag{11}$$

must be satisfied.

Writing the characteristic equations in dimensionless form facilitates the computation necessary for a numerical solution. Thus, the following dimensionless quantities are defined:

$$\left.\begin{aligned} &\bar{a}_f = \frac{a_f}{a_{f,o}} \qquad \bar{p} = \frac{p}{p_o} \qquad \bar{h} = \frac{h}{h_o} \\ &\bar{u} = \frac{u}{U_c} \qquad \bar{b} = \frac{b}{a_{f,o}t'} \qquad \bar{\rho} = \frac{\rho}{\rho_o} \\ &\bar{t} = \frac{t}{t'} \end{aligned}\right\} \tag{12}$$

The subscript o refers to the value of the quantity in the undisturbed gas before the piston is withdrawn, and U_c denotes the piston velocity required for a complete frozen

expansion to $p = 0$. The reference time t' can be chosen as necessitated by the particular expansion being calculated, with the provision that it not be zero.

These expressions are used to write the dimensionless characteristic equations of an unsteady expansion in the Lagrangian coordinate system. Along the + and - characteristic curves

$$\left.\begin{aligned}\left(\frac{d\bar{b}}{d\bar{t}}\right)_+ &= \bar{\rho}\,\bar{a}_f \\ \left(\frac{d\bar{b}}{d\bar{t}}\right)_- &= -\bar{\rho}\,\bar{a}_f\end{aligned}\right\} \tag{13}$$

the ordinary differential equations

$$\left.\begin{aligned}\frac{d\bar{u}}{d\bar{t}} + A_1\frac{1}{\bar{\rho}\,\bar{a}_f}\frac{d\bar{p}}{d\bar{t}} - A_2 t'\frac{\bar{a}_f}{\bar{\rho}\dfrac{\partial\bar{h}}{\partial\bar{\rho}}}\sum_{k=1}^{K}\frac{\partial\bar{h}}{\partial q_k}\omega_k = 0 \\ \frac{d\bar{u}}{d\bar{t}} - A_1\frac{1}{\bar{\rho}\,\bar{a}_f}\frac{d\bar{p}}{d\bar{t}} + A_2 t'\frac{\bar{a}_f}{\bar{\rho}\dfrac{\partial\bar{h}}{\partial\bar{\rho}}}\sum_{k=1}^{K}\frac{\partial\bar{h}}{\partial q_k}\omega_k = 0\end{aligned}\right\} \tag{14}$$

must be satisfied, and along the particle path

$$\left(\frac{d\bar{b}}{d\bar{t}}\right)_0 = 0 \tag{15}$$

the energy equation and the rate equations may be written as

$$\frac{d\bar{h}}{d\bar{t}} - \frac{A_3}{\bar{\rho}}\frac{d\bar{p}}{d\bar{t}} = 0 \tag{16}$$

and

$$\frac{dq_k}{d\bar{t}} = t'\omega_k \tag{17}$$

where

$$A_1 = \frac{p_o}{\rho_o a_{f,o} U_c} \qquad A_2 = \frac{a_{f,o}}{U_c} \qquad A_3 = \frac{p_o}{h_o \rho_o} \tag{18}$$

The application of the boundary conditions to the problem can be implemented by a modification of the coordinate system. This modification, first used in reference 6, is accomplished by dividing the Lagrangian particle coordinate $\bar{b}$ by the time variable $\bar{t}$ to define a new variable $\bar{y}$ – that is, $\bar{y}$ is defined by the relation

$$\bar{y} = \frac{\bar{b}}{\bar{t}} \tag{19}$$

The independent variables in the modified Lagrangian system are therefore $\bar{y}$ and $\bar{t}$. Use of such a coordinate system eliminates the singularity which exists as $\bar{t} \to 0$ and allows the boundary conditions to be applied. In addition, the network of grid points becomes more nearly rectangular in the $\bar{y},\bar{t}$ coordinates.

When $\bar{b}$ is replaced by $\overline{yt}$ in equations (13) and (15), the compatibility equations remain the same and the equations for the characteristic curves become

$$\left.\begin{aligned} \left(\frac{d\overline{yt}}{d\bar{t}}\right)_+ &= \bar{\rho}\bar{a}_f \\ \left(\frac{d\overline{yt}}{d\bar{t}}\right)_- &= -\bar{\rho}\bar{a}_f \end{aligned}\right\} \tag{20}$$

and

$$\left(\frac{d\overline{yt}}{d\bar{t}}\right)_0 = 0 \tag{21}$$

Equations (20), (14), (21), (16), and (17) make up the set of characteristic equations which, after conversion to finite-difference form, are used to obtain a numerical solution.

Boundary Conditions

Three conditions must be prescribed to determine the solution. Of these conditions, two are used in the calculation of the expansion fan and the other is used in the analysis of the near-steady region between the tail of the expansion fan and the piston face. The physical reasoning supporting the selection of the prescribed conditions is presented.

Two initial conditions are prescribed for the expansion region. First, the undisturbed gas in the reservoir is assumed to be in a state of thermodynamic equilibrium. The application of this condition in each coordinate system can be understood by considering figure 2. In $\bar{y},\bar{t}$ coordinates, this first boundary condition can be written in the form

$$\left.\begin{aligned} \bar{p}(1,\bar{t}) &= \bar{p}_o & \bar{\rho}(1,\bar{t}) &= \bar{\rho}_o \\ \bar{u}(1,\bar{t}) &= \bar{u}_o & q_k(1,\bar{t}) &= q_{k,o} \end{aligned}\right\} \tag{22}$$

The second boundary condition is obtained by considering the expansion as $\bar{t} \to 0$. A particle processed by the expansion for this second condition has a residence time which also approaches zero. The particles adjacent to the piston face experience such an expansion but, because of the short residence time, no adjustment of rate-controlled quantities occurs. It is shown mathematically in references 3 and 6 that, as $t \to 0$, the properties throughout the process are those of a frozen expansion and can be expressed as a function of $\bar{y}$. In the dimensionless modified Lagrangian coordinate system, this boundary condition may be written as

$$\left.\begin{aligned} \bar{p}(\bar{y},0) &= \bar{p}_f(\bar{y}) = \bar{y}^{\frac{2\gamma_o}{\gamma_o+1}} \\ \bar{\rho}(\bar{y},0) &= \bar{\rho}_f(\bar{y}) = \bar{y}^{\frac{2}{\gamma_o+1}} \\ \bar{u}(\bar{y},0) &= \bar{u}_f(\bar{y}) = \bar{u}_o + 1 - \bar{y}^{\frac{\gamma_o-1}{\gamma_o+1}} \\ q_k(\bar{y},0) &= q_{k,f} \end{aligned}\right\} \tag{23}$$

The values of $q_{k,f}$, of course, remain constant at the initial undisturbed values of q_k for the frozen boundary conditions.

A final boundary condition is needed to permit the calculation of the region of near-steady flow between the expansion fan and the piston face. The condition required is that the gas velocity at the piston face be the same as that of the piston. Such a condition must exist if no cavitation occurs. Cavitation, described as a breakdown in continuum flow, occurs only if the piston velocity is greater than the limiting velocity that the gas could attain in an expansion to zero pressure. Thus, by choosing the piston velocity to be less than U_c, the possibility of cavitation is eliminated.

Thermodynamic Model of Reacting Gas Mixture

The equation of state and the rate equations have been taken to be of the general forms given by equations (4) and (6), respectively. It is necessary next to develop specific relationships for the thermodynamic properties of the reacting gas and to establish detailed rate expressions for the various nonequilibrium processes.

Thermal equation of state.- The reacting gas is assumed to be made up of a mixture of perfect gases. The pressure of the mixture is equal to the sum of the partial pressures of the component species. The thermal equation of state can therefore be written as

$$p = \frac{\rho RT}{\mu} \tag{24}$$

where

$$\mu = \left(\sum_{i=1}^{n} \frac{x_i}{\mu_i} \right)^{-1} \tag{25}$$

and where R is the universal gas constant and x_i and μ_i are the mass fraction and molecular weight, respectively, of the ith species.

Internal energy.- The internal energy of the gas contains the contributions from translational, rotational, vibrational, and electronic energy modes plus the energies of dissociation and ionization. Since a mixture of perfect gases is considered, the internal energy of the mixture is equal to the sum of the internal energies of the component species. The internal energy per unit mass e can be expressed as the sum from $i = 1,. \; . \; .,n$ of the translational, rotational, vibrational, and electronic energies and the energies of dissociation and ionization.

A detailed evaluation of the contributions of the various energy modes can be made by using the appropriate partition functions. Several assumptions are made in the formulation of the expression for internal energy. The gas mixture is restricted to monatomic and diatomic species. Electronic excitation and ionization are neglected. Compositions and vibrational energies are assumed to be rate controlled. By substituting the various contributions to the internal energy into the summation equation for e, the internal energy of the reacting mixture of gases is seen to be

$$e = \sum_{i=1}^{n} \frac{x_i}{\mu_i} \left[\frac{3}{2} RT + f_i \left(RT + \sigma_i \right) + N_o \Delta_i \right] \tag{26}$$

where T is the translational temperature of the gas, N_o is the Avogadro number, and Δ_i is the heat of formation in energy per molecule for the ith specie. The factor f_i is used to permit the existence of rotational and vibrational energies for molecular species and to eliminate these energy modes for atomic species. For diatomic molecules, $f_i = 1$; for monatomic species, $f_i = 0$.

Enthalpy.- By using the definition of enthalpy

$$h = e + \frac{p}{\rho}$$

and equations (24), (25), and (26), the expression for the enthalpy in units of energy per unit mass of the mixture becomes

$$h = \sum_{i=1}^{n} \frac{x_i}{\mu_i}\left[\frac{5}{2}RT + f_i\left(\frac{p\mu}{\rho} + \sigma_i\right) + N_o\Delta_i\right] \tag{27}$$

The assumption was made previously in this analysis that the caloric equation of state could be written as equation (4) – that is, in the form

$$h = h\left(p,\rho,q_1,\ldots,q_K\right)$$

The variable q_k was used to represent all the rate-controlled variables – in this instance, the mass fraction x_i and the vibrational energy σ_i of each species of gas. Equation (27) expresses the enthalpy in the prescribed form and permits the evaluation of the enthalpy derivatives which appear in the characteristic equations.

Enthalpy derivatives.- Certain enthalpy derivatives which appear in the characteristic equations must be evaluated in terms of the gas model. The frozen speed of sound a_f, which appears in both the characteristic and the compatibility equations, is expressed in reference 13 as

$$a_f = \sqrt{\frac{\left(\frac{\partial h}{\partial \rho}\right)_{p,q_k}}{\frac{1}{\rho} - \left(\frac{\partial h}{\partial p}\right)_{\rho,q_k}}} \tag{28}$$

In order to evaluate a_f it is necessary to express $\left(\frac{\partial h}{\partial \rho}\right)_{p,q_k}$ and $\left(\frac{\partial h}{\partial p}\right)_{\rho,q_k}$ in terms of p, ρ, and q_k. By using the enthalpy expression given in equation (27), these derivatives are seen to be

$$\left.\begin{aligned}\left(\frac{\partial h}{\partial \rho}\right)_{p,q_k} &= -\sum_{i=1}^{n} \frac{x_i}{\mu_i}\left(\frac{5}{2} + f_i\right)\frac{p\mu}{\rho^2} \\ \left(\frac{\partial h}{\partial p}\right)_{\rho,q_k} &= \sum_{i=1}^{n} \frac{x_i}{\mu_i}\left(\frac{5}{2} + f_i\right)\frac{\mu}{\rho}\end{aligned}\right\} \tag{29}$$

The frozen sound speed can then be written as

$$a_f = \sqrt{\left[\frac{\sum_{i=1}^{n} \frac{x_i}{\mu_i}\left(\frac{5}{2} + f_i\right)}{\sum_{i=1}^{n} \frac{x_i}{\mu_i}\left(\frac{3}{2} + f_i\right)}\right]\frac{p}{\rho}} \tag{30}$$

It can readily be shown that the quantity in the brackets is the ratio of the frozen specific heat defined in the conventional way.

In the compatibility equations, the term $\sum_{k=1}^{K} \frac{\partial h}{\partial q_k}\omega_k$ must be evaluated. Since

$$\sum_{k=1}^{K} \frac{\partial h}{\partial q_k}\omega_k = \sum_{i=1}^{n} \frac{\partial h}{\partial x_i}\frac{dx_i}{dt} + \sum_{i=1}^{n} \frac{\partial h}{\partial \sigma_i}\frac{d\sigma_i}{dt} \tag{31}$$

expressions for the derivatives $\frac{\partial h}{\partial x_i}$ and $\frac{\partial h}{\partial \sigma_i}$ are needed. For the present gas model, these expressions are found to be

$$\frac{\partial h}{\partial x_i} = \left(\frac{5}{2} + f_i\right)\frac{p\mu}{\rho\mu_i} + \frac{f_i\sigma_i}{\mu_i} + \frac{N_o\Delta_i}{\mu_i} - \frac{\mu^2}{\mu_i}\sum_{i=1}^{n} \frac{x_i}{\mu_i}\left(\frac{5}{2} + f_i\right)\frac{p}{\rho} \tag{32}$$

and

$$\frac{\partial h}{\partial \sigma_i} = \frac{x_i f_i}{\mu_i} \tag{33}$$

When dissociative and vibrational nonequilibrium exists, the term $\sum_{k=1}^{K} \frac{\partial h}{\partial q_k}\omega_k$ may then be expressed in the following form:

$$\sum_{k=1}^{K} \frac{\partial h}{\partial q_k}\omega_k = \sum_{i=1}^{n} \left[\left(\frac{5}{2} + f_i\right)\frac{p\mu}{\rho\mu_i} + \frac{f_i\sigma_i}{\mu_i} + \frac{N_o\Delta_i}{\mu_i} - \frac{\mu^2}{\mu_i}\frac{p}{\rho}\sum_{i=1} \frac{x_i}{\mu_i}\left(\frac{5}{2} + f_i\right)\right]\frac{dx_i}{dt} + \sum_{i=1}^{n} \frac{x_i f_i}{\mu_i}\frac{d\sigma_i}{dt} \tag{34}$$

The rate equations, discussed subsequently, provide expressions for $\frac{dx_i}{dt}$ and $\frac{d\sigma_i}{dt}$ in terms of thermodynamic properties, compositions, and vibrational energies.

Rate equations.- The rate equations were postulated to take the form of equation (6) – that is,

$$\frac{dq_k}{dt} = \omega_k\left(p,\rho,q_1,\ldots,q_K\right)$$

This expression must now be expanded to more specific terms.

A rate equation is first established to describe the dissociation and recombination rates of the reacting gas species. By using the rate expression presented in reference 14 in terms of the mass fraction, the rate of change of the mass fraction of the ith species due to all reactions may be expressed as

$$\frac{dx_i}{dt} = \sum_{j=1}^{m} \frac{dx_i}{dt} = \sum_{j=1}^{m} k_j \frac{\mu_i}{\rho}\left(\nu'_{ij} - \nu_{ij}\right)\prod_{i=1}^{n}\left(\frac{x_i\rho}{\mu_i}\right)^{\nu_{ij}} \tag{35}$$

where x_i is the mass fraction of the ith species, j denotes the reaction, ν_{ij} is the stoichiometric coefficient of ith species of reactant in the jth reaction, ν'_{ij} is the stoichiometric coefficient of ith species of product in the jth reaction, and k_j is the specific reaction rate coefficient for the jth reaction. The specific reaction rate coefficient is assumed to be a function of temperature only and is an empirically determined coefficient which can be written in the following form:

$$k_j = D_j T^{E_j} \exp\left(-\frac{F_j}{T}\right) \tag{36}$$

The form of the chemical rate equation given by equation (35) is adequate for both forward and reverse reactions, provided each is treated as a separate reaction.

The adjustment of the vibrational energies toward equilibrium is also controlled by a rate process. In the present investigation, coupling between dissociation and vibrational energies is not considered. In addition, any molecule formed by the recombination process is assumed to possess the same average vibrational energy as other molecules in the flow. The vibrational rate equation may then be written as

$$\frac{d\sigma_i}{dt} = \frac{\sigma_{i,eq} - \sigma_i}{\tau_i} \tag{37}$$

where the vibrational relaxation time τ_i takes the form

$$\tau_i = \frac{A_i T^{B_i} \exp\left(\frac{C_i}{T^{1/3}}\right)}{p\left[1 - \exp\left(-\frac{\theta_i}{T}\right)\right]} \tag{38}$$

which readily fits available empirical data and agrees with the form theoretically predicted in reference 15. The equilibrium vibrational energy is assumed to be given by the expression

$$\sigma_i = \frac{R\theta_i}{\exp\left(\frac{\theta_i}{T}\right) - 1} \tag{39}$$

Vibrational-equilibrium option.- In some situations the vibrational relaxation is much more rapid than the recombination processes. It is therefore advantageous to assume vibrational equilibrium and treat the dissociation and recombination reactions as the only rate processes. For conditions considered in this investigation the variation of equilibrium vibrational energy with temperature can be represented by a series of straight lines with no appreciable loss in accuracy. Such an approximation simplifies the evaluation of enthalpy derivatives. Assuming the vibrational energy to be essentially in equilibrium permits more rapid calculation than could be attained by considering vibrational energies as rate controlled.

SOLUTION PROCEDURE

In appendix B the detailed operation of converting the nondimensionalized characteristic equations to finite-difference form and of establishing a procedure for calculating the desired flow region is presented. The calculation procedure described in appendix B was programed in FORTRAN IV language for computation on the IBM 7094 electronic data processing system. Capabilities and limitations of the program are discussed herein.

The constituents of the gas mixture must be monotomic or diatomic species if the present thermodynamic model is to be used. Conditions throughout the expansion must be such that ionization and electronic excitation can be neglected.

The program is designed to handle a number of chemical species and the associated chemical and vibrational rate equations. Computer time and storage limitations make difficult the treatment of simultaneous rate processes in which the overall rates of the important relaxation processes differ by several orders of magnitude. Since the grid size must be small enough to accommodate the fastest rate, the number of grid points required for accurate characteristic calculation places a practical limit on such work. At the present time no suitable method, comparable to the one introduced in reference 16 for

use in one-dimensional flow, has been developed for characteristic calculations. This grid-size limitation, coupled with the assumptions incorporated in the thermodynamic model, restricts the use of the computational program to fairly simple gas mixtures. These restrictions do not preclude the utilization of the program in many practical applications.

The program can be used to calculate the flow field over a large portion of the nonequilibrium region between the limiting cases of frozen and equilibrium flow. For flows expanded to very low densities, the number of grid points necessary to calculate the entire region presents a problem because of the excessive computing time required. The flow in the initial portion of the expansion reaches equilibrium rapidly; however, as the expansion proceeds, the density drops with a resulting decrease in the recombination rate. For expansions to low densities, a large region must therefore be calculated in the $\bar{t}$ direction of the $\bar{y}$-$\bar{t}$ plane to follow the flow to equilibrium. Some computational problems have been encountered in the near-equilibrium region. The procedure used in the characteristic calculation provides a natural perturbation of the nonequilibrium variables from equilibrium at the beginning of the calculation but, as calculation proceeds in the $\bar{t}$ direction and equilibrium is approached, numerical inaccuracies may occur because of the nature of the rate equations. The approach in the present investigation has been to compare the compositions and vibrational energies with the equilibrium values at the local conditions and, if they are sufficiently close, to equate all further values in the $\bar{t}$ direction to the equilibrium values. This approach has proved adequate for the simplified gas model discussed previously.

The program might be further improved by using a method similar to that presented in reference 17 to aid in the calculation of the near-equilibrium region. It might also be noted that, for many useful applications of the program, the calculations do not have to be carried to the equilibrium limit.

The program may be used for expansions in which the pressure drop does not exceed two orders of magnitude. For most applications of current interest, the rate-controlled quantities will have essentially frozen or become insignificant for this degree of expansion and any further expansion can be approximated by frozen flow.

Results calculated for the region of expanding flow may be printed out in two different ways. The thermodynamic properties, velocities, vibrational energies, and mass fractions can be printed either at each grid point in the $\bar{y}$-$\bar{t}$ plane or along specified particle paths. A numerical integration routine is also included to calculate the distance traveled by the specified particles.

RESULTS AND DISCUSSION

Results of Sample Calculation

Calculation of the unsteady expansion of a gas experiencing chemical and vibrational nonequilibrium was made for a specific set of initial conditions. Results are presented to demonstrate the utility of the computational program and to point out the salient features of such an expansion.

A simplified air model, made up of N_2, O_2, and O, is used in the analysis. The oxygen dissociation-recombination reaction

$$O_2 + M \rightleftharpoons 2O + M$$

where M is O, O_2, or N_2, is assumed to control the change in chemical composition. Different rate constants may be used for each catalytic species M. The chemical rate constants required in equation (36) were obtained from reference 18 and are listed in table I.

Rate equations of the form given by equation (37) are used to describe the relaxation of the vibrational energies of molecular oxygen and nitrogen. The vibrational-relaxation-time constants were obtained by curve fitting the values of reference 19 and are given in table II. Recent experiments described in references 20 and 21 indicate that vibrational relaxation rates in expanding N_2 and air can be expected to be 15 times as fast as those observed in compressive flows. Oxygen vibrational deexcitation, however, was measured in an unsteady expansion (ref. 5) and the results were found to agree with calculations made by using rates measured in a compressive flow. Some question exists, therefore, as to the correct rate data to use in the present investigation. Although the data of reference 19 predict rates which are possibly too slow in this expanding-flow situation, they are used herein to illustrate the handling of simultaneous vibrational and chemical rate processes. Use of the faster rates would result in vibrational equilibrium throughout the expansion. No exchange of vibrational energies between N_2 and O_2 molecules, as discussed for compressive flow in reference 22, is considered in the present study. The further assumption is made that no coupling exists between the chemical and vibrational rate processes.

The undisturbed gas, before being processed by the expansion, was assumed to exist in a state of chemical equilibrium at a temperature of 3500° K and a pressure of 1.0968×10^6 dynes/cm^2. For such conditions, the mass fraction of NO is small, the amount of N is negligible, and the other assumptions used in the formulation of the gas model are met. The simplified air model therefore appears adequate for the present application.

Variations in compositions, vibrational energies, and flow properties along specified particle paths through the unsteady expansion are presented in figures 3 to 8. The reduced time coordinate t/t_o, used as the abscissa in these figures, is obtained by dividing the actual time the particle spent in the expansion by the time at which that particle would have entered a frozen expansion. Property values along different particle paths for a given value of t/t_o describe particles which have different residence times in the expansion but which have been processed by approximately the same fraction of the total expansion. Specific particle paths are designated by t_o, the time the particle enters the fan. This value is also a direct measurement of the initial distance of the particle from the center of the expansion at time zero. Equilibrium properties are calculated by the procedure described in reference 23.

Composition changes.- The nature of the variation in composition, as depicted in figure 3, is considered. As the value of t_o of the particles increases (an indication of increased residence time in the expansion), the amount of recombination increases and thus the mass fraction of atomic oxygen in the flow decreases. The atomic oxygen decreases very rapidly during the initial part of the expansion and then levels off as if it were asymptotically approaching a constant value. This phenomenon is similar to the composition freezing which occurs in hypersonic nozzles and can be attributed basically to two factors. First, a decrease in oxygen atoms decreases the recombination rates. As recombination occurs, the mass fraction of atomic oxygen in the flow decreases. The recombination rates, which are proportional to the square or cube of the mass fraction of atomic oxygen, therefore decrease rapidly. The second factor influencing the recombination rates is the density. As expansion occurs, the density drops rapidly. From the chemical rate equation, it is apparent that the recombination rate is proportional to the square of the density. Thus, a density decrease produces a rapid decrease in the rate of recombination. This rate decrease due to density change more than offsets the effect produced by the inverse temperature dependence of the reaction rate coefficients. The net result of the property changes produced by the expanding flow on the recombination rates is a sizable reduction in these rates.

Vibrational deexcitation.- The variations in the vibrational energies of molecular nitrogen and of molecular oxygen are displayed in figures 4 and 5, respectively. Again a tendency toward freezing is noted as the gases expand to low densities. Of particular interest is the behavior of the oxygen vibrational energy. The initial rate of deexcitation is faster for the particle with the smaller residence time. The flow conditions experienced by this particle are far from equilibrium with respect to dissociation and nitrogen vibrational energy. Very little chemical or vibrational energy has been returned to the flow. The flow, therefore, possesses a low translational temperature causing the value of the term $\sigma_{i,eq} - \sigma_i$ in the oxygen vibrational rate equation to be large and thereby

providing the necessary potential for producing rapid oxygen vibrational deexcitation. As the expansion proceeds, the pressure-dependent relaxation time begins to dominate the oxygen vibrational energy relaxation, and the tendency toward freezing begins. The particle more distant from the corner has more residence time for relaxation and thus its vibrational energies approach the frozen state more slowly.

Thermodynamic properties.- The translational temperature is the thermodynamic property influenced to the greatest extent by the existence of nonequilibrium. Figure 6 shows the temperature profiles along various particle paths through the unsteady expansion. As recombination and deexcitation of vibrational energy modes occur, energy is returned to the flow and manifests itself partially in the form of a rise in translational temperature. Temperature is therefore seen to be highly dependent upon the chemical and vibrational state of the gas. The pressure variation along specified particle paths is displayed in figure 7. For a high degree of expansion, the nonequilibrium static pressure can deviate appreciably from the equilibrium value and can serve as an indicator of the degree of nonequilibrium of the flow. Density variation is not shown graphically because of its slight sensitivity to the chemical and vibrational state of the gas.

Velocity variation.- The flow velocity is of considerable interest in many applications of the unsteady expansion, particularly in those dealing with the design of facilities for producing high-velocity, high-enthalpy flow. The effect of the chemical state of the gas on the velocity is therefore very important. It can be seen from figure 8 that, as the recombination increases, the velocity of the gas increases. This increase in velocity is to be expected inasmuch as some of the energy released by the recombination is converted into flow energy. In order for the maximum velocity to be obtained in an unsteady expansion, the process must take place in a state of chemical equilibrium.

Proposed Applications of Program

The practical flow situations which can be calculated by using the present computational program can be divided into two basic categories. The sample calculation just presented provides an example of the first category. This category of application deals with the determination of the effects of nonequilibrium on the unsteady expansion of a gas being processed for use as a test medium. The objectives of the analysis are to predict flow-property variations through the expansion and to ascertain the state of the test gas. Temperature and pressure ranges must be restricted to conform with the assumptions of the thermodynamic model. The number of species and reactions considered must be held to a minimum to make computation practical. For many problems of this nature, such as the analysis of expansion-tube flow (ref. 1), these restrictions do not prohibit realistic calculation.

The second category in which the present program can be utilized is the analysis of unsteady expansions in kinetic rate studies. The use of the unsteady expansion in producing conditions for which recombination and vibrational relaxation can be measured is described in references 3, 4, and 5. An experiment of this kind would be performed with a mixture containing a large percent of an inert gas such as argon and a smaller amount of a gas such as nitrogen or oxygen for which the rate is to be measured. The present program is well suited for calculating such a flow. The calculations would be used to predict the ideal test conditions for the experiment and would provide the basis for comparison between measured and calculated values needed to determine actual values of rate constants.

CONCLUDING REMARKS

A procedure, based on the method of characteristics applied in a Lagrangian frame of reference, has been presented for calculating the centered one-dimensional unsteady expansion of a multicomponent gas mixture subject to chemical and vibrational nonequilibrium. A computer program was developed to perform the calculation on the IBM 7094 electronic data processing system. The results from a sample calculation are presented to show the utility of the program and to illustrate the pertinent features of a nonequilibrium unsteady expansion.

Langley Research Center,
National Aeronautics and Space Administration,
Langley Station, Hampton, Va., September 2, 1966,
129-01-08-16-23.

APPENDIX A

DERIVATION OF CHARACTERISTIC EQUATIONS

Nonequilibrium Characteristics

Equations (1), (2), (3), and (6), written in Lagrangian coordinates, describe the one-dimensional unsteady flow of a reacting gas mixture. This system of equations is hyperbolic in nature and therefore has real valued characteristics. The equations defining the characteristic curves and compatibility relations are developed in this appendix by using these basic governing equations. In order to simplify the ensuing manipulations, only one of the rate-controlled variables q_k is considered and is denoted simply as q. It is apparent subsequently that this simplification does not limit the generality of the development of the characteristic equations.

First, the caloric equation of state, equation (4), is used to eliminate derivatives of ρ. This equation may be written in the following form:

$$\frac{\partial h}{\partial t} = \left(\frac{\partial h}{\partial p}\right)_{\rho,q} \frac{\partial p}{\partial t} + \left(\frac{\partial h}{\partial \rho}\right)_{p,q} \frac{\partial \rho}{\partial t} + \left(\frac{\partial h}{\partial q}\right)_{p,\rho} \frac{\partial q}{\partial t} \tag{A1}$$

By introducing the energy equation, equation (3), and the frozen-sound-speed expression, equation (28), equation (A1) can be rearranged to give

$$\frac{\partial \rho}{\partial t} = \frac{1}{a_f^2} \frac{\partial p}{\partial t} - \frac{\left(\frac{\partial h}{\partial q}\right)_{p,\rho} \frac{\partial q}{\partial t}}{\left(\frac{\partial h}{\partial \rho}\right)_{p,q}} \tag{A2}$$

Equation (1) can then be written as

$$\frac{\partial u}{\partial b} + \frac{\rho_o}{\rho^2 a_f^2} \frac{\partial p}{\partial t} - \frac{\rho_o}{\rho^2} \frac{\left(\frac{\partial h}{\partial q}\right)_{p,\rho} \frac{\partial q}{\partial t}}{\left(\frac{\partial h}{\partial \rho}\right)_{p,q}} = 0 \tag{A3}$$

Since p, u, h, and q are functions of the independent variables b and t, the following equations may be written:

$$dp = \frac{\partial p}{\partial b} db + \frac{\partial p}{\partial t} dt \tag{A4}$$

APPENDIX A

$$du = \frac{\partial u}{\partial b}\,db + \frac{\partial u}{\partial t}\,dt \tag{A5}$$

$$dh = \frac{\partial h}{\partial b}\,db + \frac{\partial h}{\partial t}\,dt \tag{A6}$$

$$dq = \frac{\partial q}{\partial b}\,db + \frac{\partial q}{\partial t}\,dt \tag{A7}$$

Characteristic curves for the set of governing equations – that is, equations (2), (3), (6), (A3), (A4), (A5), (A6), and (A7) – can exist only if the determinant of the matrix of coefficients of this set is equal to zero. The characteristic directions are obtained by equating the following determinant of coefficients to zero and evaluating it for that condition:

From equation:	$\frac{\partial h}{\partial b}$	$\frac{\partial h}{\partial t}$	$\frac{\partial u}{\partial b}$	$\frac{\partial u}{\partial t}$	$\frac{\partial q}{\partial b}$	$\frac{\partial q}{\partial t}$	$\frac{\partial p}{\partial b}$	$\frac{\partial p}{\partial t}$
(A6)	db	dt	0	0	0	0	0	0
(3)	0	1	0	0	0	0	0	$-\frac{1}{\rho}$
(A5)	0	0	db	dt	0	0	0	0
(2)	0	0	0	1	0	0	$\frac{1}{\rho_o}$	0
(A7)	0	0	0	0	db	dt	0	0
(6)	0	0	0	0	0	1	0	0
(A4)	0	0	0	0	0	0	db	dt
(A3)	0	0	1	0	0	$\left[-\frac{\rho_o}{\rho^2}\frac{\left(\frac{\partial h}{\partial q}\right)_{p,\rho}}{\left(\frac{\partial h}{\partial \rho}\right)_{p,q}}\right]$	0	$\frac{\rho_o}{\rho^2 a_f^2}$

$= 0$ (A8)

This equation reduces to

$$\left(\frac{db}{dt}\right)^2\left[\left(\frac{db}{dt}\right)^2 - \frac{\rho^2 a_f^2}{\rho_o^2}\right] = 0 \tag{A9}$$

It should be noted that, for each additional value of q considered, the factor $\frac{db}{dt}$ is raised to one higher power. An increase in the number of rate processes considered does not, therefore, introduce any additional characteristic directions.

By setting each factor of equation (A9) equal to zero, the characteristic directions are seen to be

$$\left.\begin{aligned}\left(\frac{db}{dt}\right)_+ &= \frac{\rho a_f}{\rho_o} \\ \left(\frac{db}{dt}\right)_- &= -\frac{\rho a_f}{\rho_o}\end{aligned}\right\} \tag{A10}$$

and

$$\left(\frac{db}{dt}\right)_0 = 0 \tag{A11}$$

Equations (A10) and (A11) are given in the text as equations (7) and (9).

The compatibility relations which apply along these characteristic curves may now be easily obtained. Along the directions in equation (A10), equations (2) and (A3) can be combined to produce the following ordinary differential equations:

$$\left.\begin{aligned}\frac{du}{dt} + \frac{1}{\rho a_f}\frac{dp}{dt} - \frac{a_f}{\rho}\frac{\frac{\partial h}{\partial q}\frac{\partial q}{\partial t}}{\frac{\partial h}{\partial \rho}} &= 0 \\ \frac{du}{dt} - \frac{1}{\rho a_f}\frac{dp}{dt} + \frac{a_f}{\rho}\frac{\frac{\partial h}{\partial q}\frac{\partial q}{\partial t}}{\frac{\partial h}{\partial \rho}} &= 0\end{aligned}\right\} \tag{A12}$$

Equation (A12) is expressed in the text as equation (8).

Along the particle path given by $\left(\frac{db}{dt}\right)_0 = 0$, the energy equation and the rate equation become

$$\frac{dh}{dt} - \frac{1}{\rho}\frac{dp}{dt} = 0 \tag{A13}$$

and

$$\frac{dq}{dt} = \omega(p,\rho,q) \tag{A14}$$

respectively. In the text, equation (A13) is given as equation (10) and equation (A14) is given in more general form as equation (11).

It is interesting to compare the characteristic equations presented with similar equations for a perfect gas. The perfect-gas characteristics show that, along the lines given in equation (A10), the compatibility relations are

$$\left.\begin{aligned} \frac{du}{dt} \pm \frac{1}{\rho a}\frac{dp}{dt} = 0 \\ \frac{du}{dt} - \frac{1}{\rho a}\frac{dp}{dt} = 0 \end{aligned}\right\} \tag{A15}$$

In the nonequilibrium expansion the frozen speed of sound a_f assumes the role of the perfect-gas unambiguous sound speed a, so the directions of the nonequilibrium and perfect-gas characteristic lines are similar. The compatibility equations, however, are not of identical form because of the addition in the nonequilibrium expansion of the term which is due to the inclusion of rate processes in the formulation of the problem.

Frozen Characteristics

In the limiting case of frozen flow, the rate-controlled quantities have no time in which to relax, q_k is constant, and therefore $\omega_k = 0$. The frozen flow then reduces to the perfect-gas expansion in which the frozen compositions and vibrational energies are used in the calculation of the sound speed.

Equilibrium Characteristics

If the flow is to remain in thermodynamic equilibrium throughout the expansion, all rate processes must be assumed to occur infinitely fast. The characteristic equations for the equilibrium expansion cannot be obtained as a limiting case of the nonequilibrium process since the rate equations become indeterminate. The characteristic equations can be developed separately for the mathematical model of equilibrium. The equilibrium characteristic equations are equivalent to the characteristic equations for a perfect gas with a perfect-gas sound speed replaced by the local equilibrium speed of sound a_{eq}.

APPENDIX B

NUMERICAL CALCULATION PROCEDURE

The calculation procedure presented in this appendix closely follows the method outlined in reference 7. It consists of the conversion of the characteristic equations to finite-difference form and the establishment of a step-by-step computational scheme.

Finite-Difference Form of Characteristic Equations

When the nomenclature of figure 9 and second-order finite-difference approximations are used, the equations for the characteristic curves given by equation (20) become

$$\bar{y}_P\bar{t}_P - \bar{y}_A\bar{t}_A = \left[\bar{\rho}\,\bar{a}_f\right]_{AP}\left(\bar{t}_P - \bar{t}_A\right) \tag{B1}$$

and

$$\bar{y}_P\bar{t}_P - \bar{y}_B\bar{t}_B = -\left[\bar{\rho}\,\bar{a}_f\right]_{BP}\left(\bar{t}_P - \bar{t}_B\right) \tag{B2}$$

and the respective compatibility relations given by equation (14) become

$$\bar{u}_P - \bar{u}_A + A_1\left[\frac{1}{\bar{\rho}\,\bar{a}_f}\right]_{AP}\left(\bar{p}_P - \bar{p}_A\right) - A_2\left(\frac{\bar{a}_f t'}{\bar{\rho}\dfrac{\partial\bar{h}}{\partial\bar{\rho}}}\sum_{k=1}^{K}\frac{\partial h}{\partial q_k}\omega_k\right)_{AP}\left(\bar{t}_P - \bar{t}_A\right) = 0 \tag{B3}$$

and

$$\bar{u}_P - \bar{u}_B - A_1\left[\frac{1}{\bar{\rho}\,\bar{a}_f}\right]_{BP}\left(\bar{p}_P - \bar{p}_B\right) + A_2\left(\frac{\bar{a}_f t'}{\bar{\rho}\dfrac{\partial\bar{h}}{\partial\bar{\rho}}}\sum_{k=1}^{K}\frac{\partial h}{\partial q_k}\omega_k\right)_{BP}\left(\bar{t}_P - \bar{t}_B\right) = 0 \tag{B4}$$

A bracketed expression denotes the average of the value of the term contained in the bracket at the two grid points denoted by the bracket subscript. In finite-difference form the particle path, equation (21), becomes simply

$$\bar{y}_P\bar{t}_P = \bar{y}_D\bar{t}_D \tag{B5}$$

Along the particle path, the energy and rate equations may be written as

APPENDIX B

$$\bar{h}_P - \bar{h}_D = A_3\left[\frac{1}{\bar{\rho}}\right]_{DP}\left(\bar{p}_P - \bar{p}_D\right) \tag{B6}$$

$$x_{i,P} - x_{i,D} = t'\left[\frac{dx_i}{dt}\right]_{DP}\left(\bar{t}_P - \bar{t}_D\right) \tag{B7}$$

and

$$\sigma_{i,P} - \sigma_{i,D} = t'\left[\frac{d\sigma_i}{dt}\right]_{DP}\left(\bar{t}_P - \bar{t}_D\right) \tag{B8}$$

Equations (B1) to (B8) form the basis of the characteristic program for obtaining a numerical solution.

Calculation Procedure for Expansion Fan

For the expansion region, the calculations are carried out in the dimensionless modified Lagrangian coordinate system. The nature of the grid used in the calculations is shown in figure 10.

From the initial conditions it is known that, along the line $\bar{t} = 0$, all conditions are those of a frozen expansion. Thus, the values of all quantities at points (M,1) are known. Also, the properties along the line $\bar{y} = 1$ are those of the undisturbed gas. Thus, all quantities are known for points (1,N). The starting point for the calculation is obviously point (2,2) inasmuch as points (2,1), (1,1), and (1,2) are known from the boundary conditions. The finite-difference equations are used to obtain the coordinates, properties, compositions, and velocities at point (2,2). Once point (2,2) has been calculated, points (2,2), (1,2), and (1,3) are used to calculate point (2,3). Thus, the calculation marches up the (2,N) line until the limiting N is reached. Then by using points (3,1), (2,1), and (2,2), point (3,2) is calculated and the same marching process is used along line (3,N). A marching process is therefore established which moves to the left after each successive column is calculated. This process continues until all desired points have been calculated.

The preceding discussion outlines the general calculation of the entire flow field. The key operation is the calculation of values at any unknown point by using the known values at three adjacent points and the finite-difference characteristic equations. This operation is an iterative process and requires a fairly elaborate calculation procedure. The following steps are used in this calculation:

1. All quantities are known at points A, B, and C (see fig. 9) from the boundary conditions or previous calculations. As a first assumption, the values of the thermodynamic properties, compositions, and velocity at point P are equated to the respective values at

point A. This assumption is accurate because, for flow with no nonequilibrium present, a simple flow region would exist and properties at points A and P would be identical. Differences in properties at points A and P are due then to nonequilibrium effects and not to the expansion process.

2. Equations (B1) and (B2) are solved simultaneously to give $\bar{y}_P$ and $\bar{t}_P$, the coordinates of point P.

3. The coordinates of point D must now be established to indicate where a particle path through point P intersects line CA or CB. This step is necessary because the rate equations and energy equations must be evaluated along the line DP. Equation (B5) gives the particle path as $\bar{y}_P\bar{t}_P = \bar{y}_D\bar{t}_D$. Three possible locations of point D must be considered. If $\bar{y}_P\bar{t}_P > \bar{y}_C\bar{t}_C$, point D is on line CB. Since for the frozen expansion CB is a straight line, it seems reasonable to treat CB as a straight line over the small interval considered herein. Writing the equation of the line CB and solving this equation simultaneously with the condition $\bar{y}_P\bar{t}_P = \bar{y}_D\bar{t}_D$ yield the values of the desired coordinates $\bar{y}_D$ and t_D. A linear interpolation between points C and B is used to obtain values of the properties, compositions, and velocity at point D. If $\bar{y}_P\bar{t}_P < \bar{y}_C\bar{t}_C$, point D is on line CA. The line CA is of the form, $\overline{yt}^2 = \text{Constant}$ for the frozen expansion, so this form appears reasonable for use herein. Thus, by assuming $\bar{y}_D\bar{t}_D^2 = \frac{1}{2}\left(\bar{y}_C\bar{t}_C^2 + \bar{y}_A\bar{t}_A^2\right)$ and by using the condition $\bar{y}_P\bar{t}_P = \bar{y}_D\bar{t}_D$, the coordinates $\bar{y}_D$ and $\bar{t}_D$ are readily found. A linear interpolation between properties at points A and C is used to evaluate the flow quantities at point D. If $\bar{y}_P\bar{t}_P = \bar{y}_D\bar{t}_D$, points D and C are identical and properties at D are defined.

4. The rate expressions for the rate processes considered are evaluated at points A, B, P, and D for use in the compatibility and rate equations. Thus $\frac{dx_i}{dt}$ and $\frac{d\sigma_i}{dt}$ can be calculated for all species by using equations (35) and (37).

5. The compatibility equations, equations (B3) and (B4), are solved simultaneously to obtain improved values of $\bar{p}_P$ and $\bar{u}_P$. The value of $\bar{t}_P$ is determined by step 1.

6. Rate equations (B7) and (B8) are applied along the particle path from point D to point P to obtain improved values of x_i and σ_i at point P.

7. The finite-difference form of the energy equation, equation (B6), is applied along particle path DP to yield the following new value of $\bar{h}_P$:

$$\bar{h}_P = \bar{h}_D + \frac{2A_3\left(\bar{p}_P - \bar{p}_D\right)}{\left(\bar{\rho}_D + \bar{\rho}_P\right)} \tag{B9}$$

8. A new temperature at point P, found by using the definition of enthalpy, is

$$T_P = \frac{\bar{h}_0 \bar{h}_P - \sum_{i=1}^{n} \frac{x_{i,P}}{\mu_i}\left(f_i \sigma_{i,P} + N_0 \Delta_i\right)}{R \sum_{i=1}^{n} \frac{x_{i,P}}{\mu_i}\left(\frac{5}{2} + f_i\right)} \tag{B10}$$

9. The thermal equation of state is utilized to calculate an improved density at point P.

10. Improved values are thus available for the thermodynamic properties, compositions, and velocity at point P. The improved values are used with the previously assumed values in a second-order correction scheme to obtain an improved approximation of the values at point P. The calculation returns to step 2 and the procedure is repeated with these new values. The iteration process continues until successive calculated values are within a prescribed degree of agreement. Inasmuch as temperature is more sensitive to nonequilibrium effects than other properties, successive temperature values are compared to establish the convergence of the iteration. When successive values are within a prescribed range of agreement, the calculation proceeds to the next grid point.

Calculation of Near-Steady Region

A calculation procedure has been established for computing the flow in the expansion fan. The near-steady region, the region between the tail of the expansion fan and the piston face, may also be calculated by using the same procedure with slight modifications. Two significant changes are necessary. First, it is convenient to use the $\bar{b},\bar{t}$ coordinate system instead of the $\bar{y},\bar{t}$ coordinate system. This change affects only the equations specifying the characteristic directions. Second, the boundary condition of constant-velocity flow is imposed at grid points on the piston face. At these points, $\bar{u}_P$ is fixed and equation (B4) is adequate for obtaining an improved value of $\bar{p}_P$; thus step 5 of the calculation procedure is unnecessary. Interior points are calculated by using essentially the same procedure as that used for the expansion fan.

REFERENCES

1. Trimpi, Robert L.: A Preliminary Theoretical Study of the Expansion Tube, a New Device for Producing High-Enthalpy Short-Duration Hypersonic Gas Flows. NASA TR R-133, 1962.

2. Spurk, Joseph H.: Design, Operation and Preliminary Results of the BRL Expansion Tube. Rept. No. 1304, Ballistic Res. Labs., Aberdeen Proving Ground, Oct. 1965.

3. Connor, Laurence Neuman, Jr.: The One-Dimensional Unsteady Expansion of a Reacting Mixture of Gases Considering Vibrational and Chemical Nonequilibrium. Ph. D. Thesis, North Carolina State Univ., 1965.

4. Jacobs, T. A.; Hartunian, R. A.; Giedt, R. R.; and Wilkins, R.: Direct Measurements of Recombination Rates in a Shock Tube. Phys. Fluids, vol. 6, no. 7, July 1963, pp. 972-974.

5. Holbeche, T. A.: Spectrum-Line-Reversal Temperature Measurements Through Unsteady Rarefaction Waves in Vibrationally Relaxing Oxygen. Nature, vol. 203, no. 4944, Aug. 1, 1964, pp. 476-479.

6. Wood, William W.; and Parker, F. R.: Structure of a Centered Rarefaction Wave in a Relaxing Gas. Phys. Fluids, vol. 1, no. 3, May-June 1958, pp. 230-241.

7. Appleton, J. P.: The Structure of a Centered Rarefraction Wave in an Ideal Dissociating Gas. A.A.S.U. Rept. No. 136, Univ. of Southampton, April 1960.

8. Arave, R. J.; and Brown, E. A.: Centered Rarefraction Wave in a Chemically Reacting Gas. Rept. No. D2-22534, Boeing Co., 1963.

9. Lighthill, M. J.: Dynamics of a Dissociating Gas. Part I – Equilibrium Flow. J. Fluid Mech., vol. 2, pt. 1, Jan. 1957, pp. 1-32.

10. Freeman, N. C.: Non-Equilibrium Flow of an Ideal Dissociating Gas. J. Fluid Mech., vol. 4, pt. 4, Aug. 1958, pp. 407-425.

11. Connor, Laurence N., Jr., and Taylor, Frances W.: The Centered One-Dimensional Unsteady Expansion of a Vibrationally Relaxing Nitrogen-Oxygen Mixture. NASA TN D-3805, 1967.

12. Courant, R.; and Friedrichs, K. O.: Supersonic Flow and Shock Waves. Interscience Publ., Inc. (New York), 1948.

13. Vincenti, Walter G.; and Kruger, Charles H., Jr.: Introduction to Physical Gas Dynamics. John Wiley and Sons, Inc., c.1965.

14. Penner, S. S.: Chemistry Problems in Jet Propulsion. Pergamon Press, 1957.

15. Landau, L.; and Teller, E.: Theory of Sound Dispersion. Phys. Zeitschr. der Sowjetunion, vol. 10, no. 1, 1936, pp. 34-43.

16. Treanor, Charles E.: A Method for the Numerical Integration of Coupled First-Order Differential Equations With Greatly Different Time Constants. Math. Computation, vol. 20, no. 93, Jan. 1966, pp. 39-45.

17. Pearson, Walter E.; and Baldwin, Barrett S., Jr.: A Method for Computing Nonequilibrium Channel Flow of a Multicomponent Gaseous Mixture in the Near-Equilibrium Region. NASA TN D-3306, 1966.

18. Wray, Kurt L.: Chemical Kinetics of High Temperature Air. Hypersonic Flow Research, Frederick R. Riddell, ed., Academic Press (New York), 1962, pp. 181-204.

19. Blackman, Vernon: Vibrational Relaxation in Oxygen and Nitrogen. J. Fluid Mech., vol. 1, pt. 1, May 1956, pp. 61-85.

20. Hurle, I. R.; Russo, A. L.; and Hall, J. Gordon: Spectroscopic Studies of Vibrational Nonequilibrium in Supersonic Nozzle Flows. J. Chem. Phys., vol. 40, no. 8, Apr. 1964, pp. 2076-2089.

21. Sebacher, Daniel I.: An Electron Beam Study of Vibrational and Rotational Relaxing Flows of Nitrogen and Air. Paper presented at the 1966 Heat Transfer and Fluid Mechanics Institute (Santa Clara, Calif.), June 22-24, 1966.

22. White, Donald R.; and Millikan, Roger C.: Vibrational Relaxation in Air. AIAA J., vol. 2, no. 10, Oct. 1964, pp. 1844-1846.

23. Grose, William L.; and Trimpi, Robert L.: Charts for the Analysis of Isentropic One-Dimensional Unsteady Expansions in Equilibrium Real Air With Particular Reference to Shock-Initiated Flows. NASA TR R-167, 1963.

TABLE I.- CHEMICAL RATE CONSTANTS

(a) Dissociation reactions

Constant	Value for reaction –		
	$O_2 + O \rightarrow 3O$	$O_2 + O_2 \rightarrow O_2 + 2O$	$O_2 + N_2 \rightarrow N_2 + 2O$
D_j, $cm^3/mole\text{-}sec$	0.905×10^{20}	0.3258×10^{20}	0.724×10^{19}
E_j, $cm^3/mole\text{-}sec$	-1.0	-1.0	-1.0
F_j, $cm^3/mole\text{-}sec$	59 395	59 395	59 395

(b) Recombination reactions

Constant	Value for reaction –		
	$3O \rightarrow O_2 + O$	$O_2 + 2O \rightarrow 2O_2$	$N_2 + 2O \rightarrow O_2 + N_2$
D_j, $cm^6/mole^2\text{-}sec$	0.75417×10^{17}	0.2715×10^{17}	0.60334×10^{16}
E_j, $cm^6/mole^2\text{-}sec$	-0.5	-0.5	-0.5
F_j, $cm^6/mole^2\text{-}sec$	0	0	0

TABLE II.- VIBRATIONAL CHARACTERISTIC TEMPERATURE AND RATE CONSTANTS

Constant	Value for species –	
	O_2	N_2
θ_i, ^oK	2270	3390
A_i, atm-sec	0.1424	560.61
B_i	0.3718	-0.0995
C_i	179.33	163.63

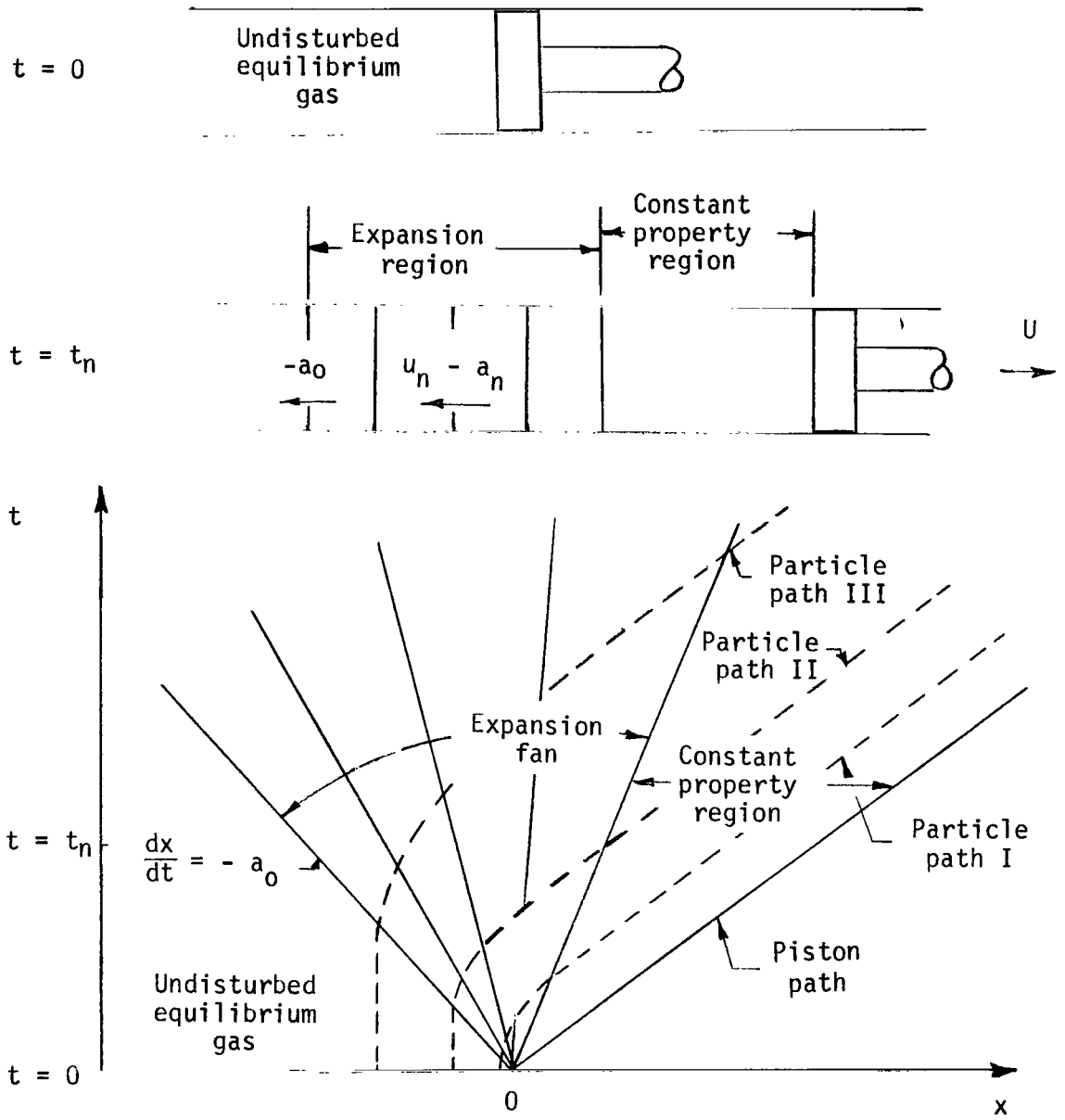

Figure 1.- Distance-time diagram of an unsteady expansion.

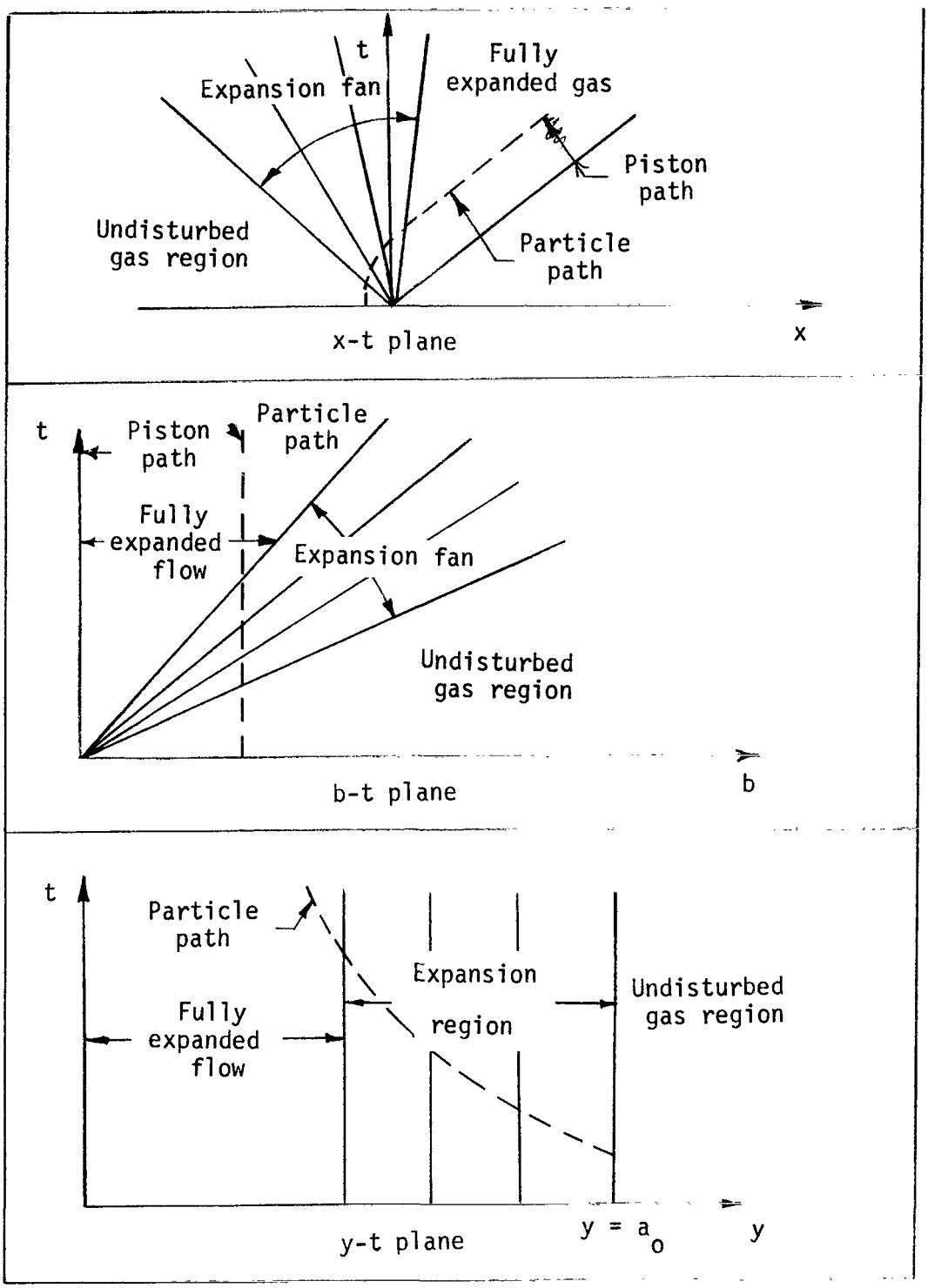

Figure 2.- Boundary conditions in the three coordinate systems.

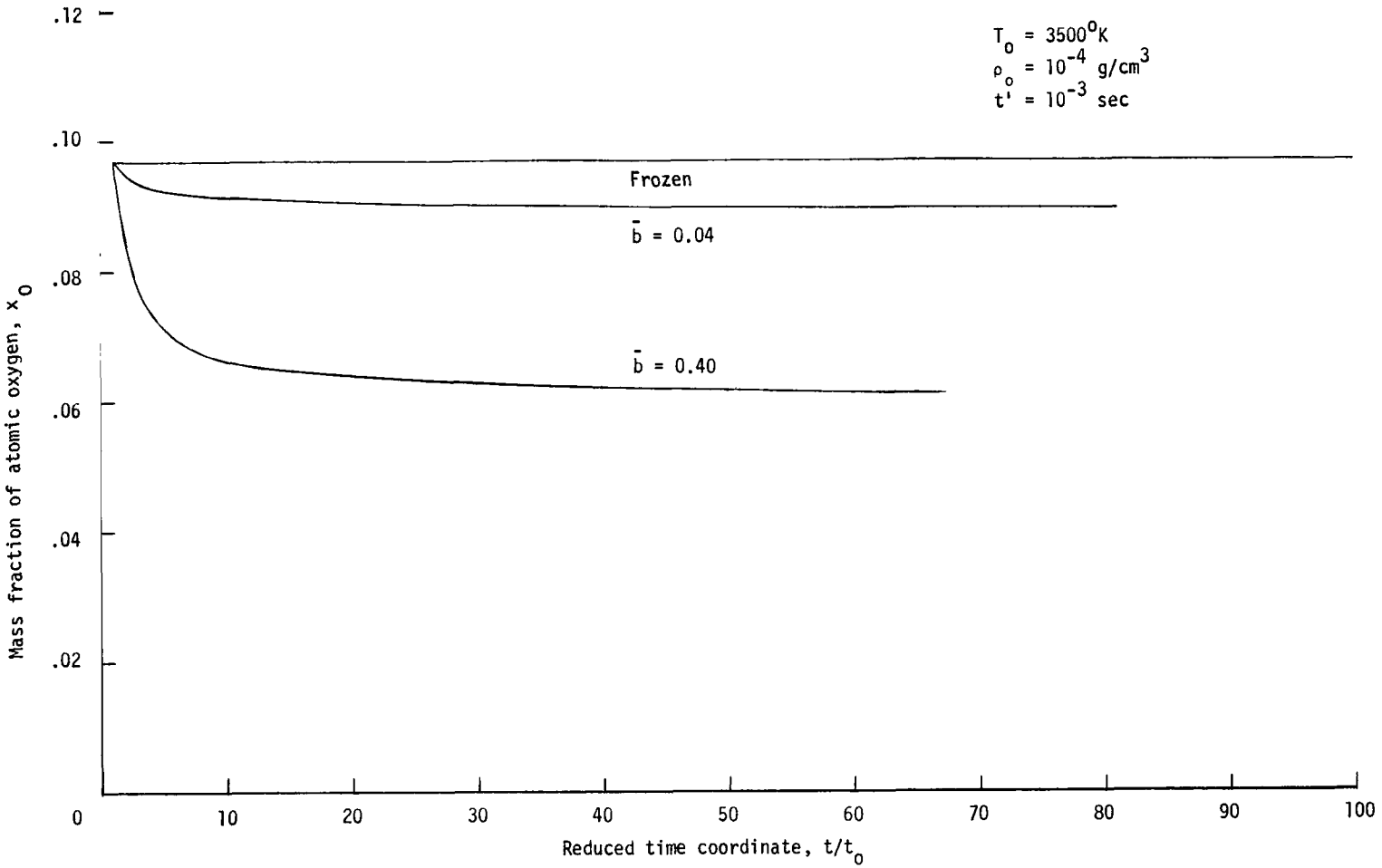

Figure 3.- Variation of the mass fraction of atomic oxygen along specific particle paths in an unsteady expansion.

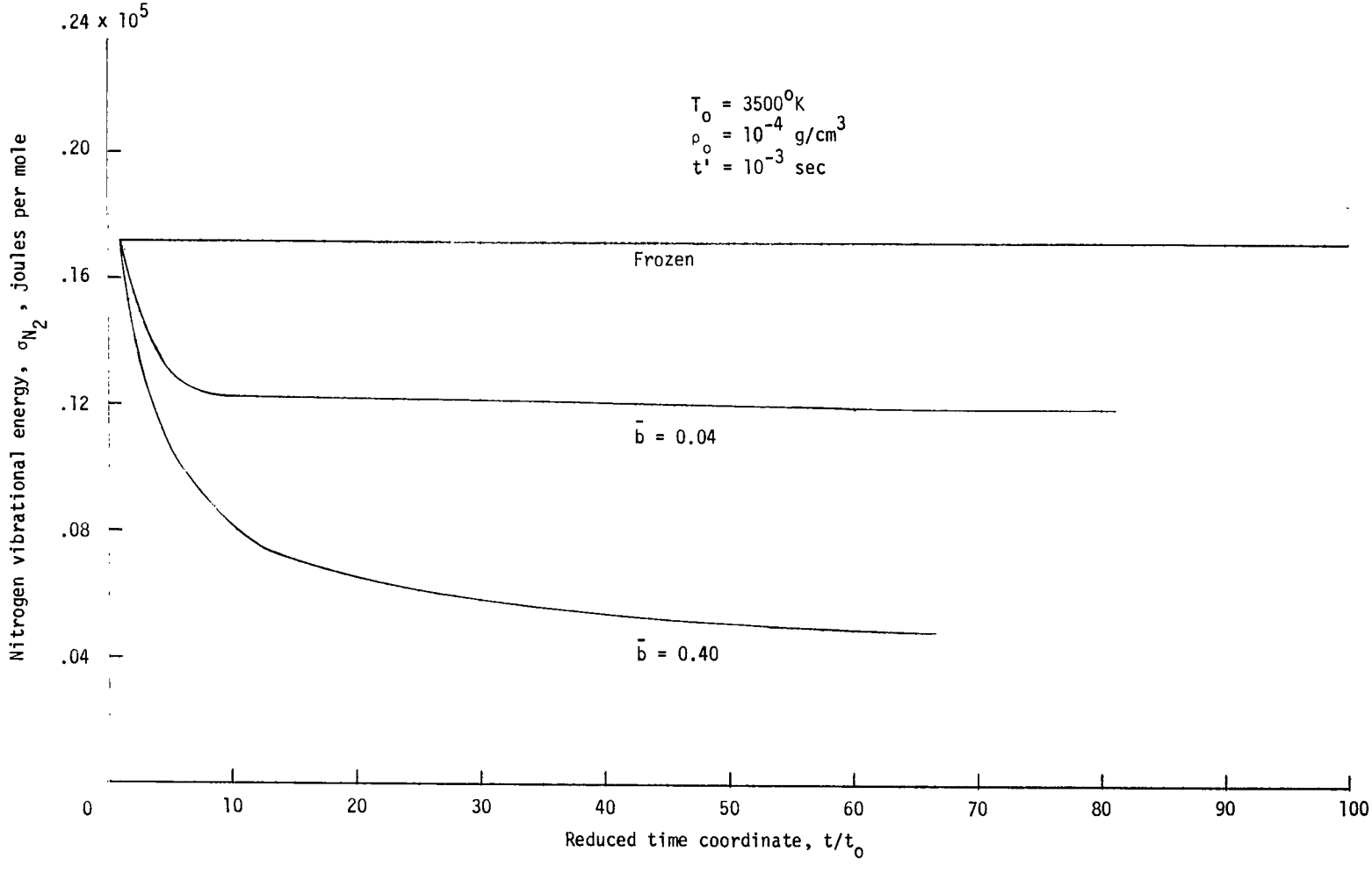

Figure 4.- Variation of the nitrogen vibrational energy along specific particle paths in an unsteady expansion.

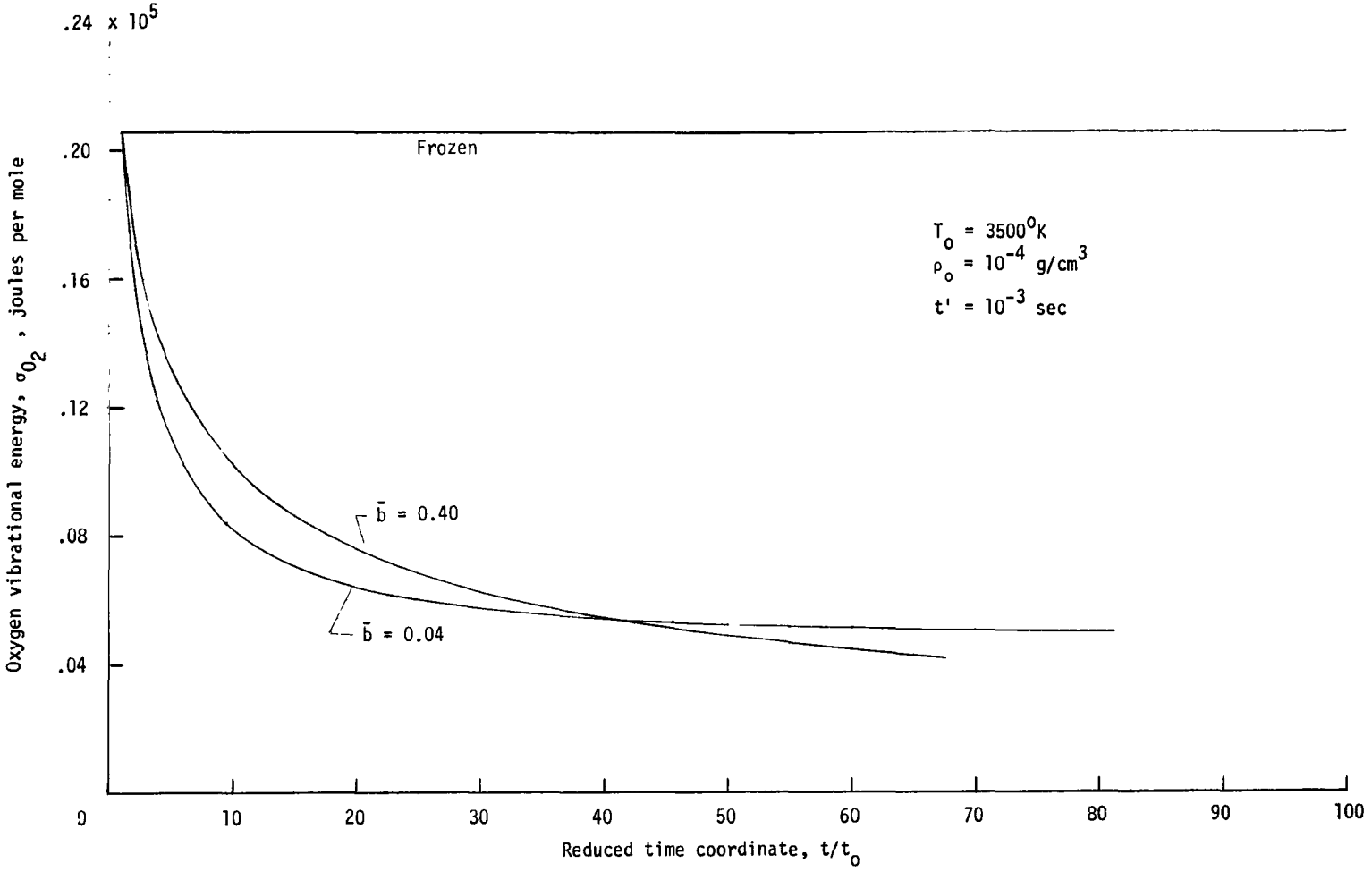

Figure 5.- Variation of the oxygen vibrational energy along specific particle paths in an unsteady expansion.

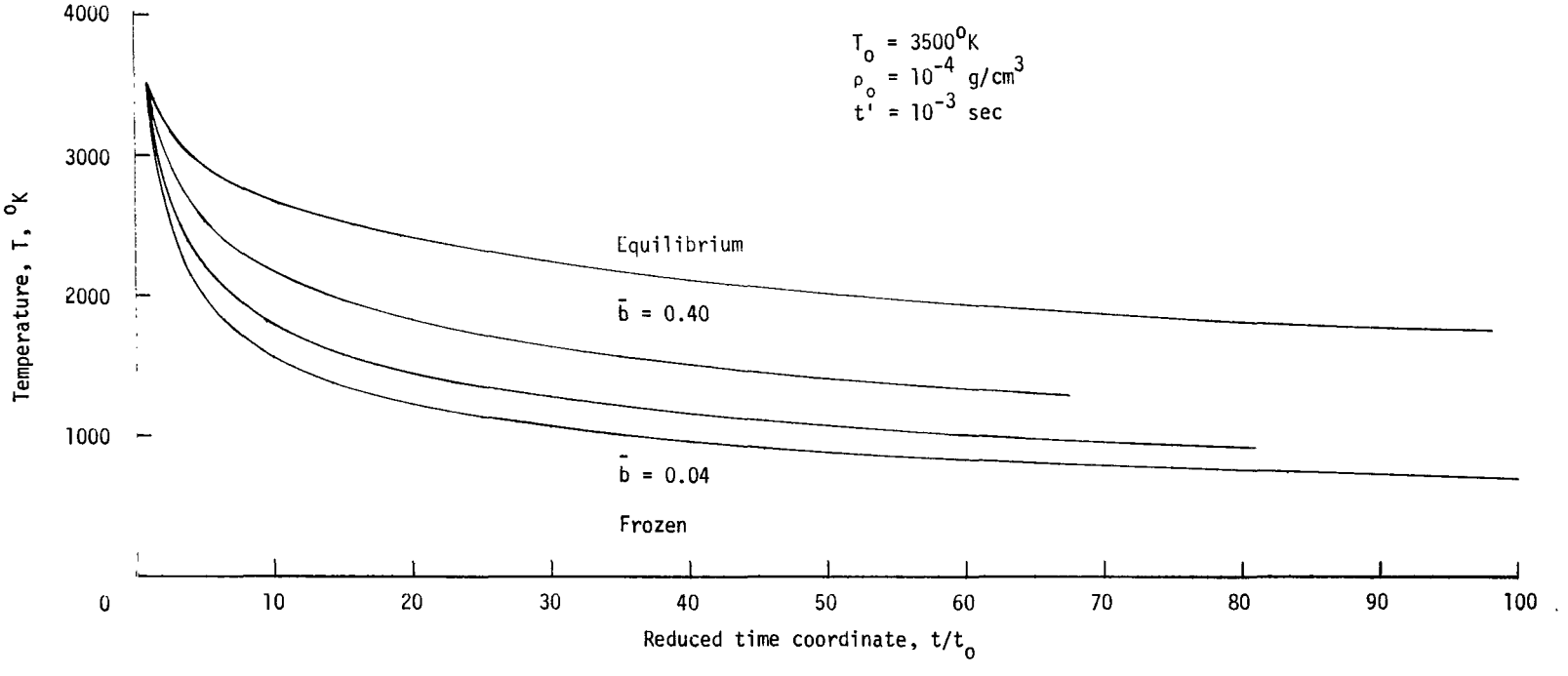

Figure 6.- Temperature variation along specific particle paths in an unsteady expansion.

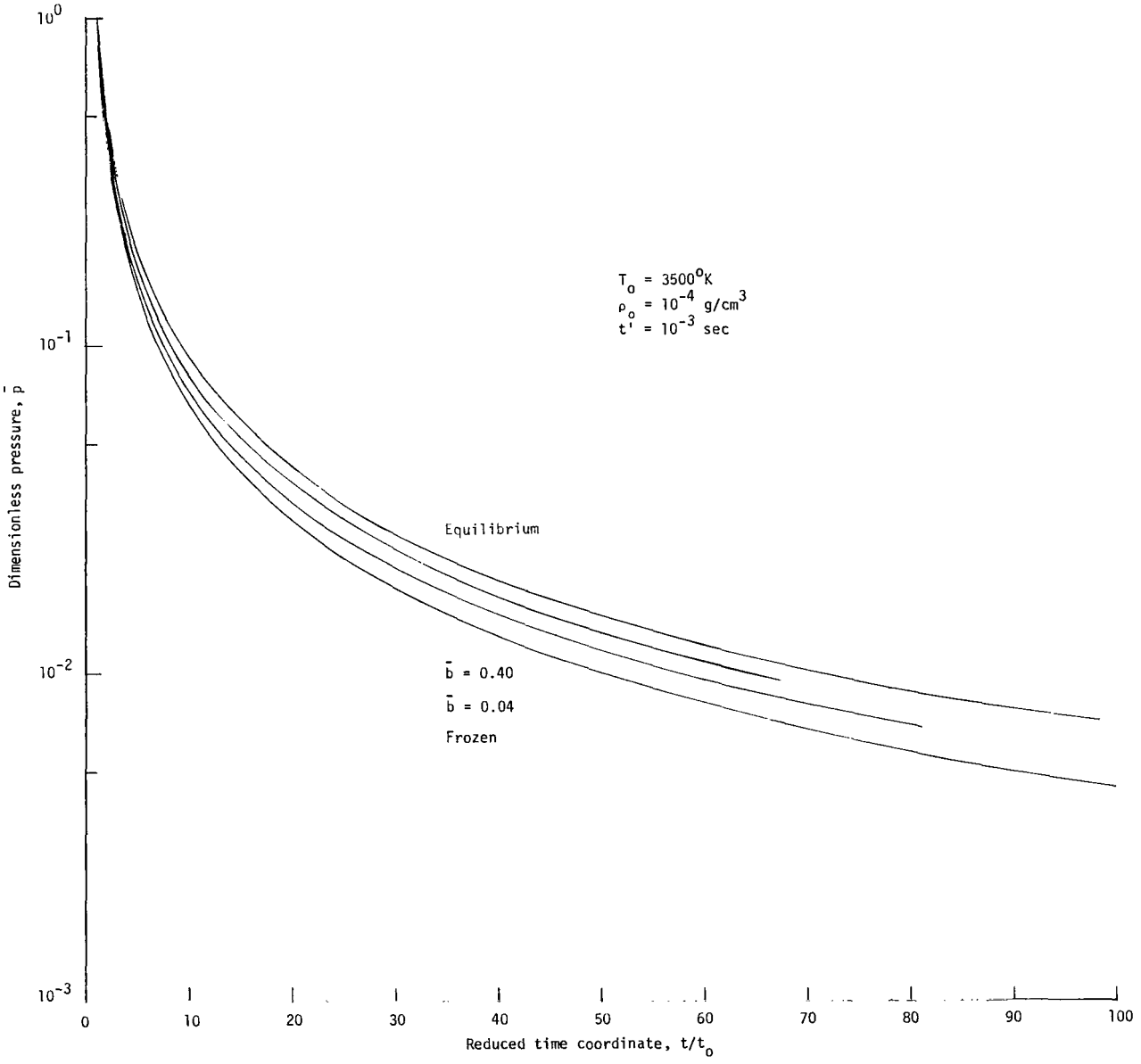

Figure 7.- Pressure variation along specific particle paths in an unsteady expansion.

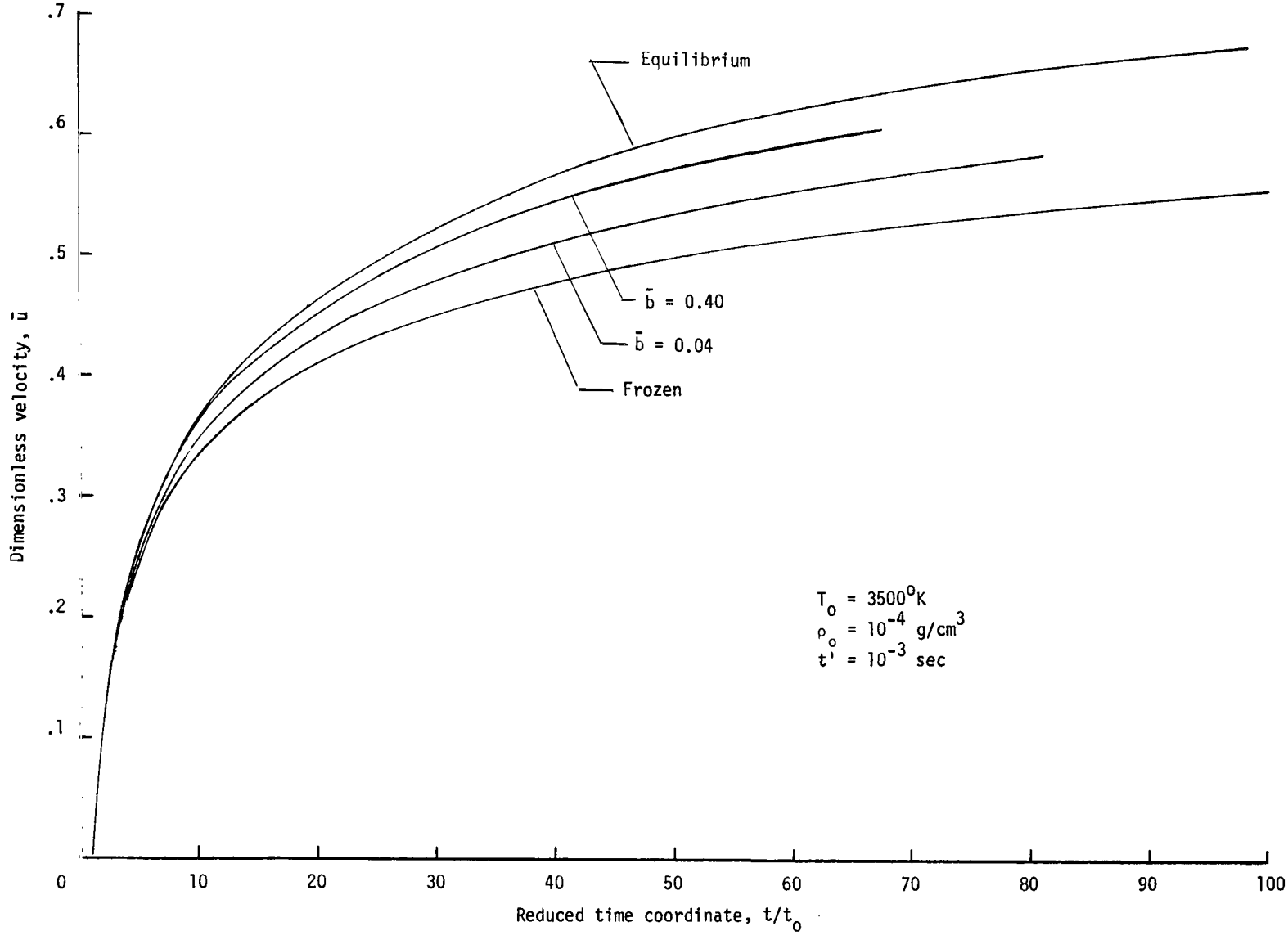

Figure 8.- Velocity variation along specific particle paths in an unsteady expansion.

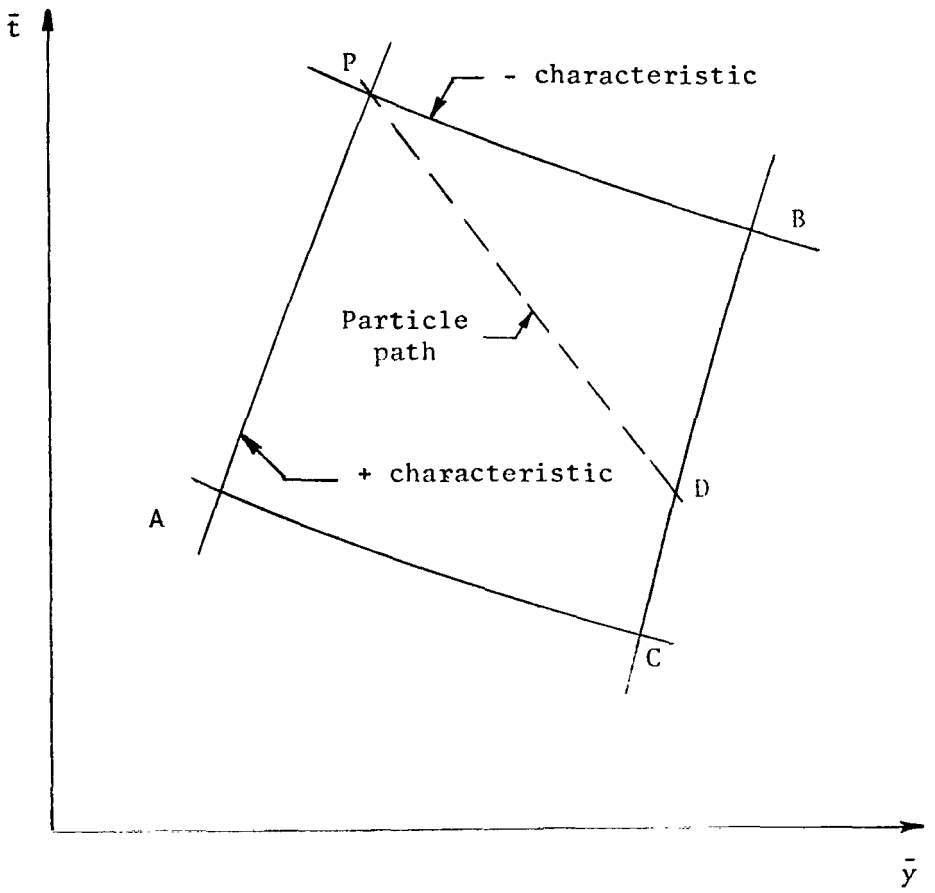

Figure 9.- General grid nomenclature.

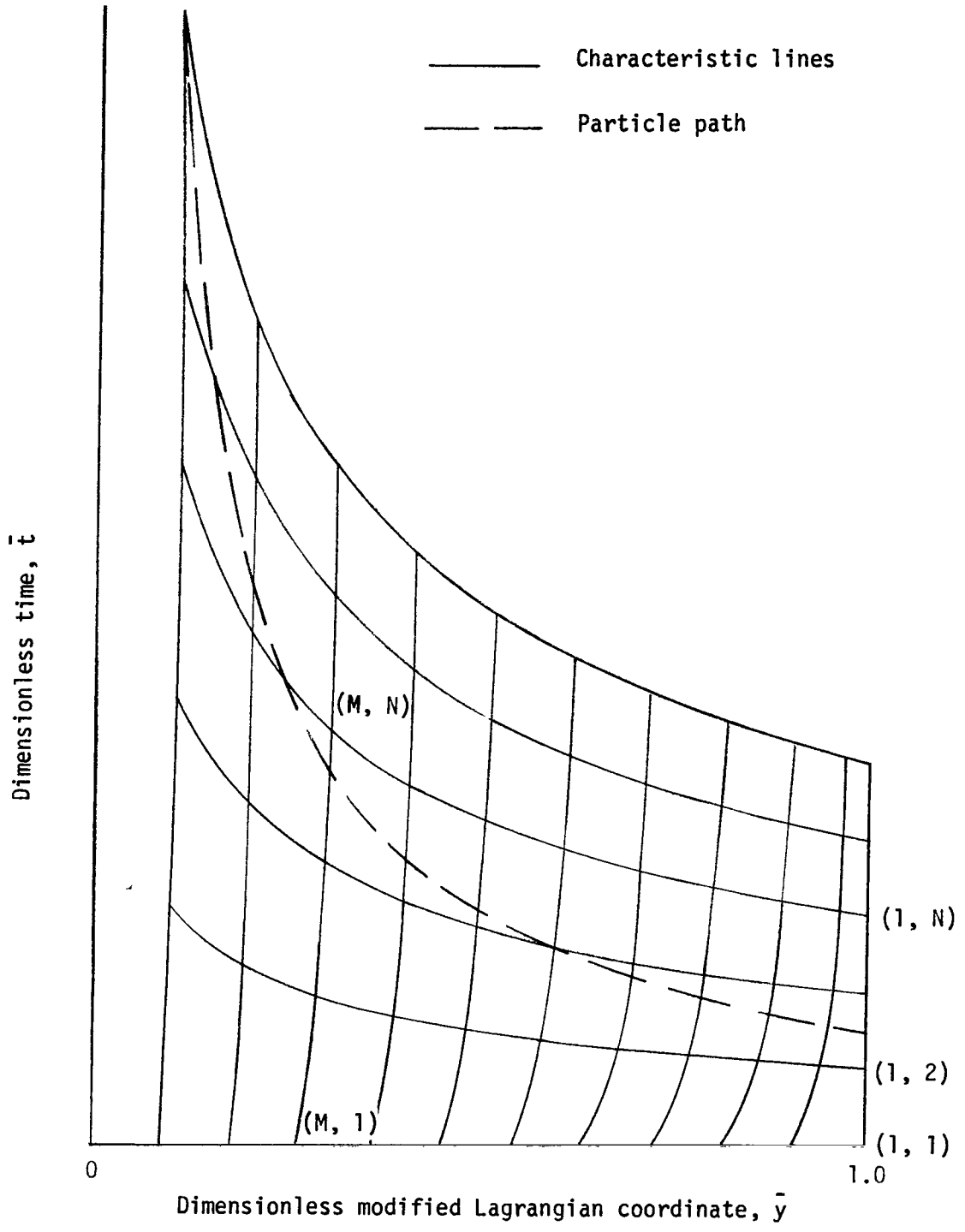

Figure 10.- Complete grid network. (M,N) denotes a general point.

"The aeronautical and space activities of the United States shall be conducted so as to contribute . . . to the expansion of human knowledge of phenomena in the atmosphere and space. The Administration shall provide for the widest practicable and appropriate dissemination of information concerning its activities and the results thereof."

—NATIONAL AERONAUTICS AND SPACE ACT OF 1958

NASA SCIENTIFIC AND TECHNICAL PUBLICATIONS

TECHNICAL REPORTS: Scientific and technical information considered important, complete, and a lasting contribution to existing knowledge.

TECHNICAL NOTES: Information less broad in scope but nevertheless of importance as a contribution to existing knowledge.

TECHNICAL MEMORANDUMS: Information receiving limited distribution because of preliminary data, security classification, or other reasons.

CONTRACTOR REPORTS: Technical information generated in connection with a NASA contract or grant and released under NASA auspices.

TECHNICAL TRANSLATIONS: Information published in a foreign language considered to merit NASA distribution in English.

TECHNICAL REPRINTS: Information derived from NASA activities and initially published in the form of journal articles.

SPECIAL PUBLICATIONS: Information derived from or of value to NASA activities but not necessarily reporting the results of individual NASA-programmed scientific efforts. Publications include conference proceedings, monographs, data compilations, handbooks, sourcebooks, and special bibliographies.

Details on the availability of these publications may be obtained from:

SCIENTIFIC AND TECHNICAL INFORMATION DIVISION

NATIONAL AERONAUTICS AND SPACE ADMINISTRATION

Washington, D.C. 20546